Appendix E

Inversion Statistics

The information in Appendix E was developed under the guidance of Dr. Russell Schnell of the Environmental Research Laboratory, Boulder, Colorado; Dr. John Kahl, University of Wisconsin/Milwaukee; and Dr. Mark Serreze, University of Colorado, Boulder.

The maps (Figs. E-1 through E-20) are statistical representations of inversions in the North Polar region. The database used to derive the maps contains soundings for 0000 GMT and 1200 GMT for the regularly reporting stations north of 60 °N in Eurasia, Alaska, Canada, and Greenland for the years 1976 to 1987. Some U.S.S.R. drifting station data were also used.

The stations were selected to achieve maximum spatial coverage with the most data possible at each station. (A list follows the figures.) Some stations have complete data for the time span while most others have at least 50 percent availability each year for at least 10 of the 12 years of record. Two exceptions were Khatanga and Zyrianka, both in the U.S.S.R.; these stations had the 50 percent criterion for 8 years and 5 years, respectively. They were included to gain better coverage over the Taimyr Peninsula and Eastern Siberia. The drifting station data were obtained from three U.S.S.R. North Pole (NP) series of manned camps (NP-22, NP-26, and NP-28). Data from NP-26 and NP-28 were available intermittently from November 1983 through December 1987, with a nearly complete record for July 1986 through December 1987. Station NP-22 reported data from May 1979 through February 1982.

Quality control checks were made by passing the data through a limits check with loose bounds to identify obviously erroneous values. Soundings were then inspected to ensure that geopotential heights increased and pressures decreased upward. Further errors were eliminated during processing to obtain the inversion statistics. Only $\approx 0.1\%$ of all data were found to contain errors.

The focus here is on low-level inversions, defined as those with a base below the 700-mb level. Inversions are identified using the detection algorithm developed by Kahl (1990). Each temperature profile is scanned upwards from the surface to the 700-mb level to locate the first layer (if any) in which temperature decreases with altitude. Thin (< 100 m) negative-lapse layers are occasionally encountered in the upward scan. If the next layer above shows an increase in temperature with altitude, the thin layer is considered to be embedded within the overall inversion layer. Examples of the technique are given by Kahl.

The statistics are defined as follows:

(1) Frequency of inversions (%): The percentage of all valid soundings in which an inversion was present.

(2) Frequency of elevated inversions (%): The percentage of all valid soundings in which an elevated inversion (i.e., an inversion with a mixed layer below the inversion base) was present.

(3) Median inversion depth (Z): The depth of the inversion layer, defined as the difference (in meters) between the inversion top and inversion base. Both elevated and ground-based inversions are included in this statistic.

(4) Median temperature difference across the inversion layer (T): The median temperature difference from the inversion top to the inversion base. Both elevated and ground-based inversions are included.

(5) Inversion intensity: This statistic, defined as T^2/Z, was originally defined by Belmont (1958) in similar form as T^2/P (P being pressure) as an overall measure of inversion strength. Clearly T itself is a valid measure of inversion strength. However, while two different inversions may have a similar T, their relative importance is increased by weighting T with Z, thus highlighting the greater temperature gradient. Both elevated and ground-based inversions are included in calculating this statistic.

In the maps the seasons are defined as follows: winter (Jan-Mar), spring (Apr-Jun), summer (Jul-Sep) and autumn (Oct-Dec). Drifting station location is defined as the midpoint along the station trajectory for each season of each year. The maps were contoured using a computer graphics package with some subsequent manual adjustments. The location of the fixed stations are shown by dots. Solid contours are used for areas over land and in the marginal seas where the data are fairly extensive, while dashed contours are used for areas within the pack ice north of the land stations where the interpolations are mostly determined by the relatively sparse drifting station data.

Eureka, Northwest Territories and Verkhoyansk, U.S.S.R. are located in valleys where cold-air drainage apparently occurs. Data from these stations showed extremely high intensity inversion values, which resulted in the computer-generated contours depicting "bullseyes." These two stations were eventually eliminated from the data set that produced the contours, and their intensity values are identified on the maps as local maxima.

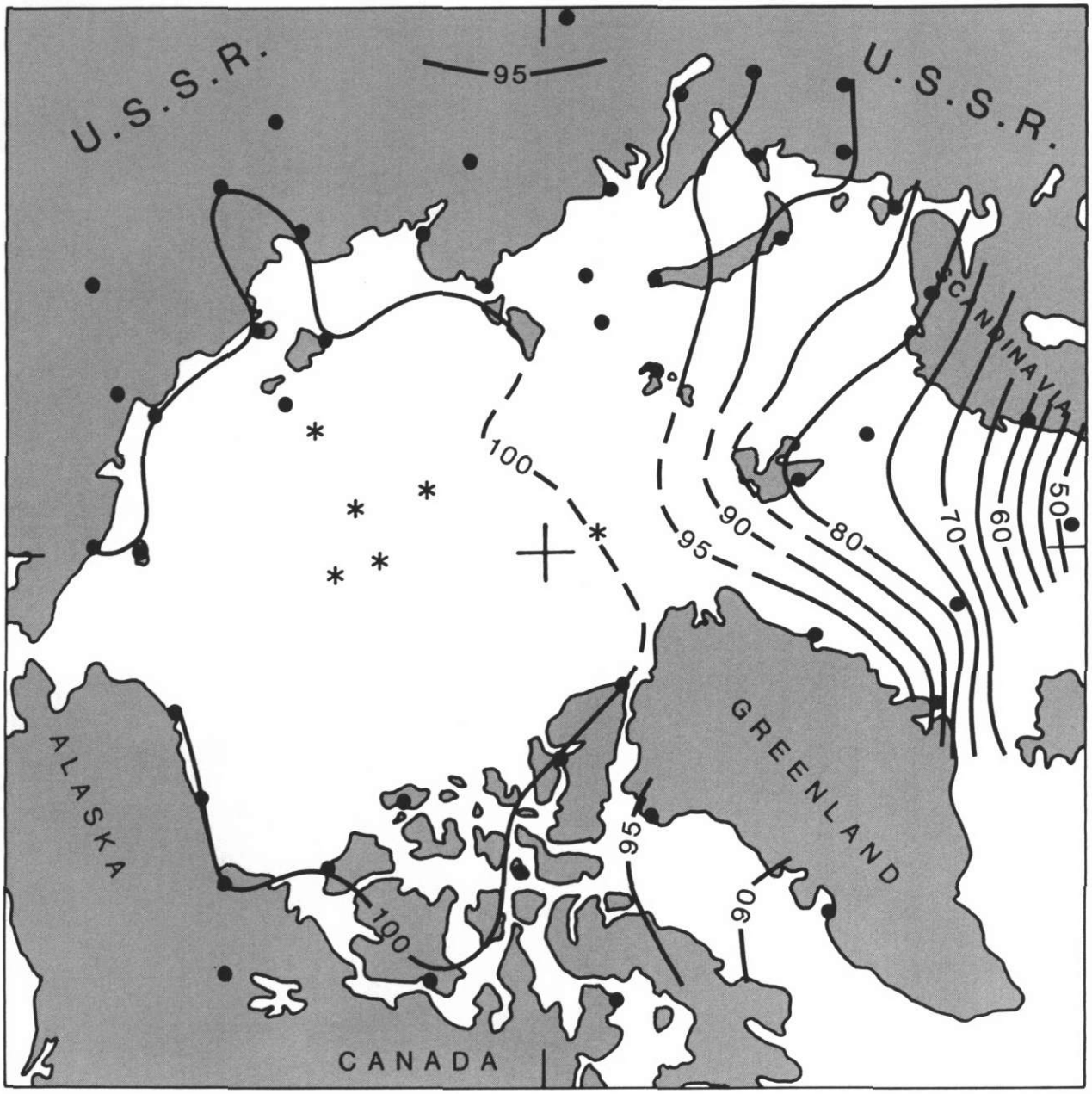

Figure E-1. Frequency of Inversions (%) for Winter.

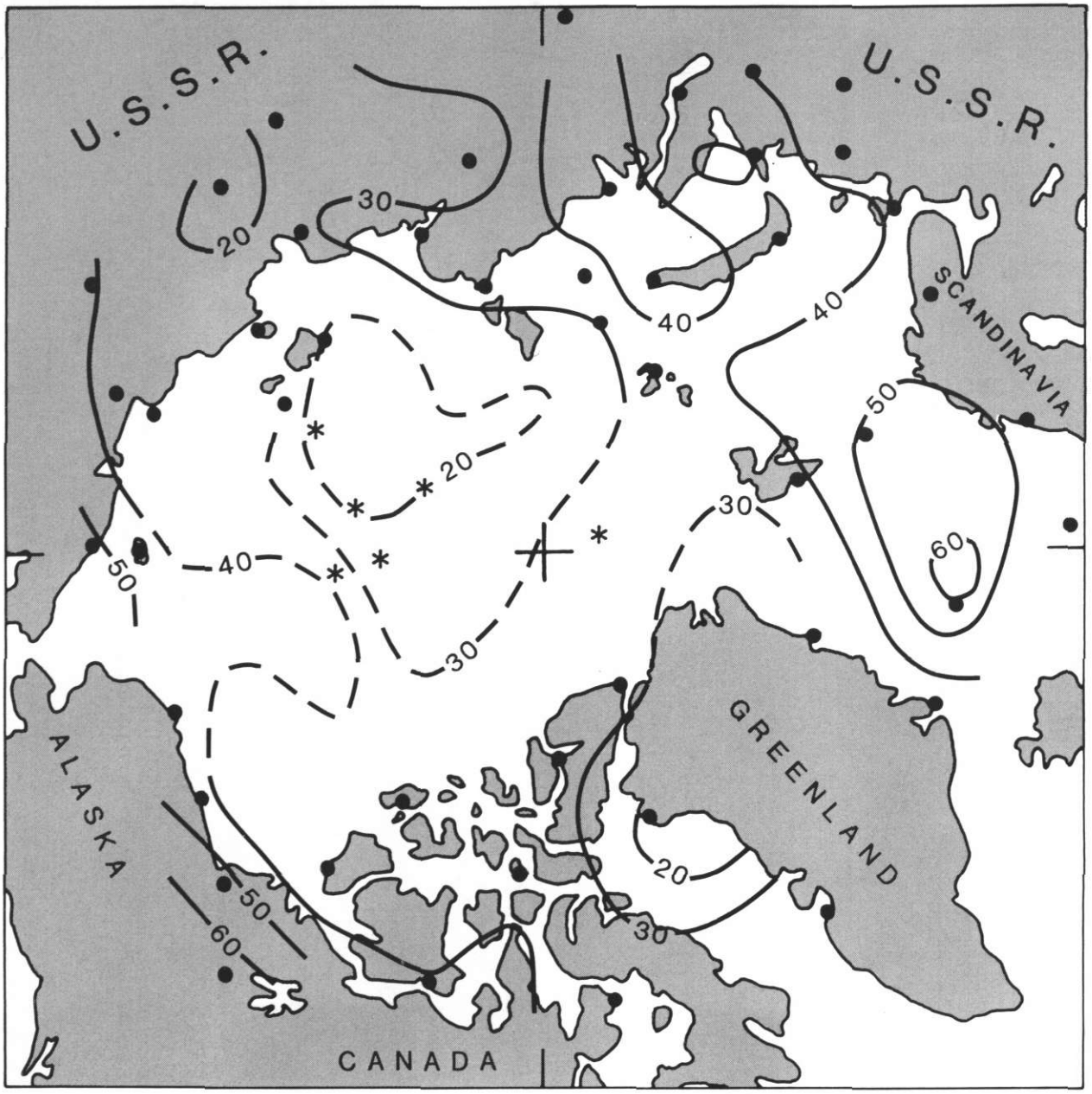

Figure E-2. Frequency of Elevated Inversions (%) for Winter.

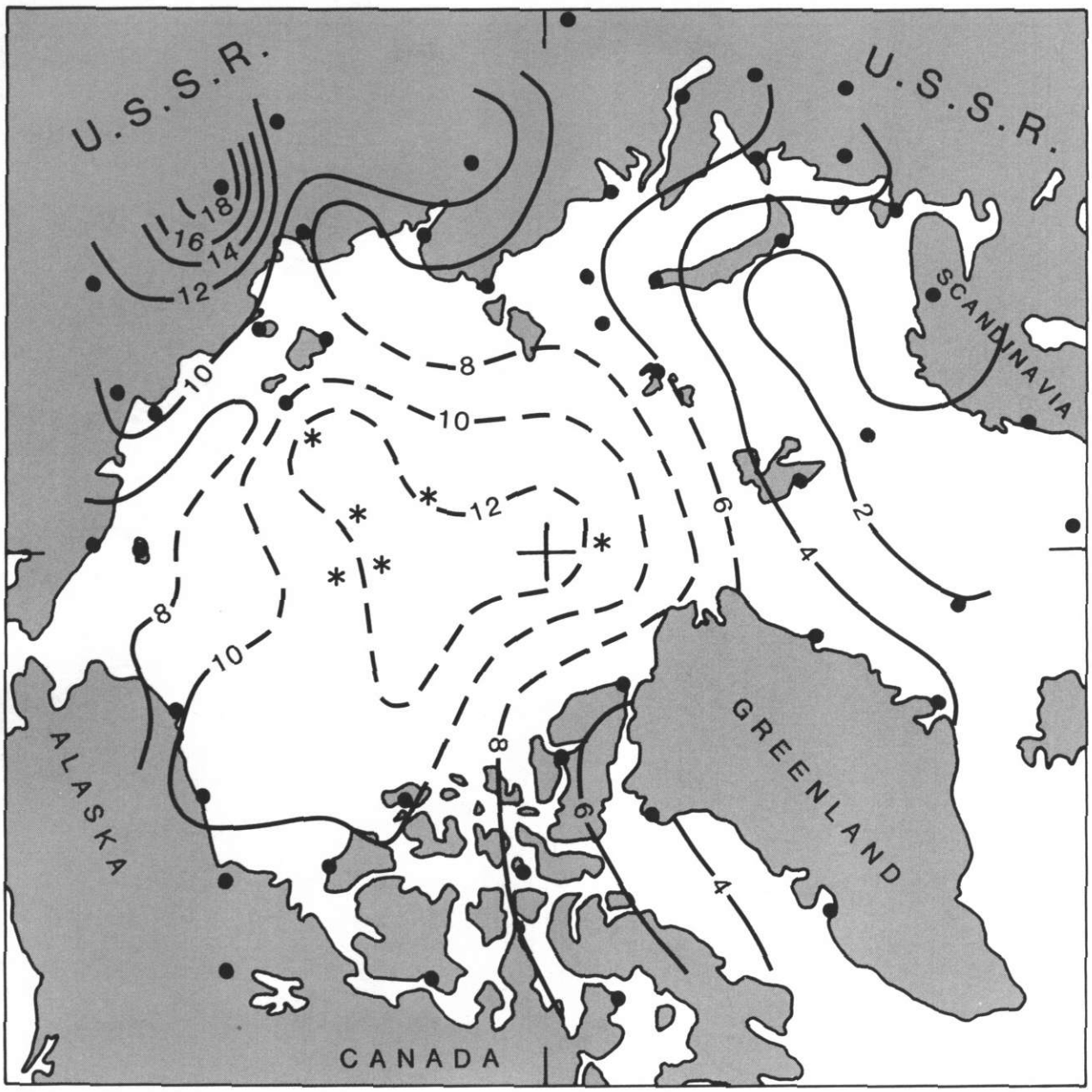

Figure E-3. Median Temperature Difference Across Inversion (°C) for Winter.

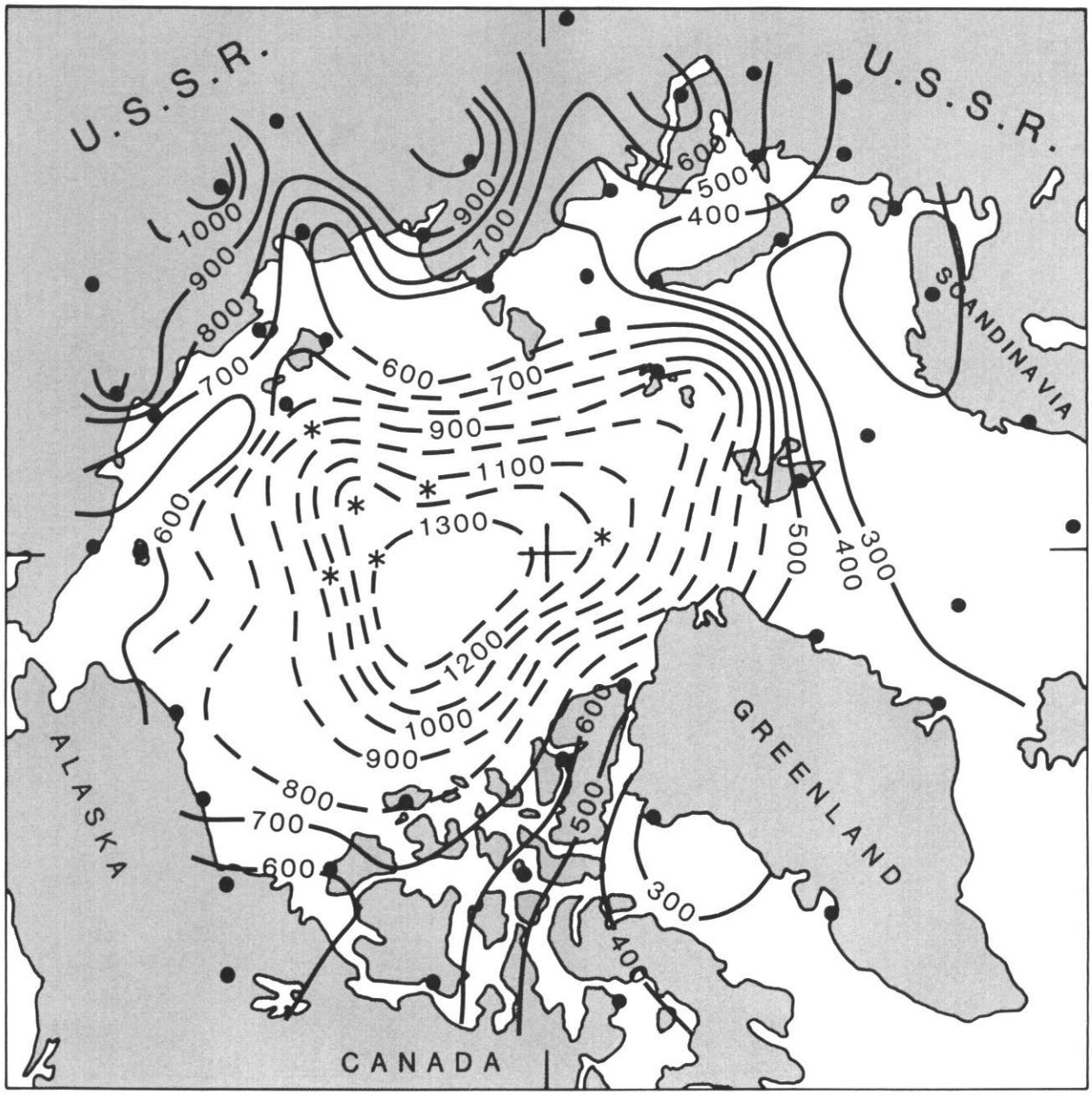

Figure E-4. Median Inversion Depth (m) for Winter.

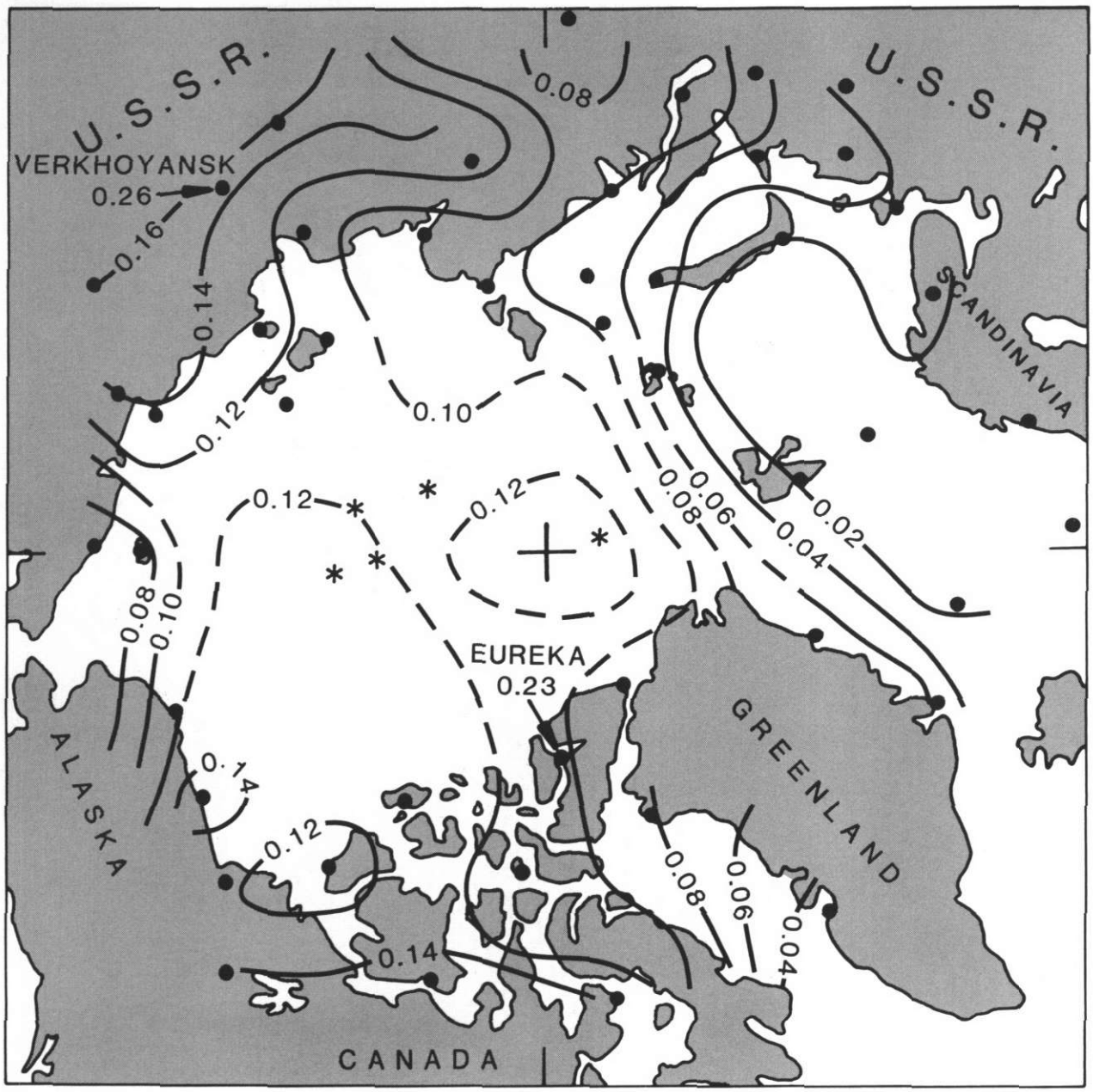

Figure E-5. Median Inversion Intensity ($\Delta T^2/m$) for Winter.

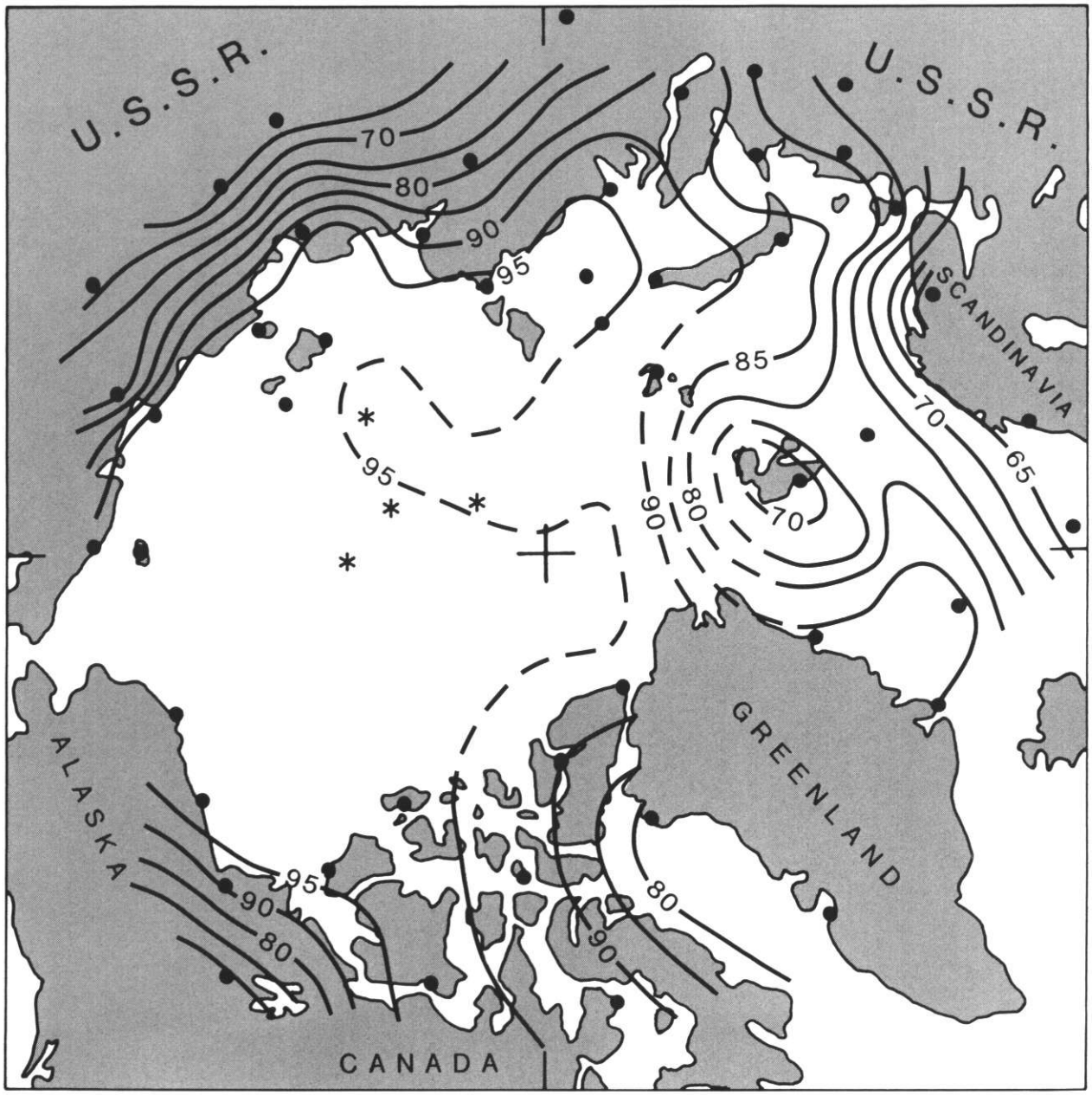

Figure E-6. Frequency of Inversions (%) for Spring.

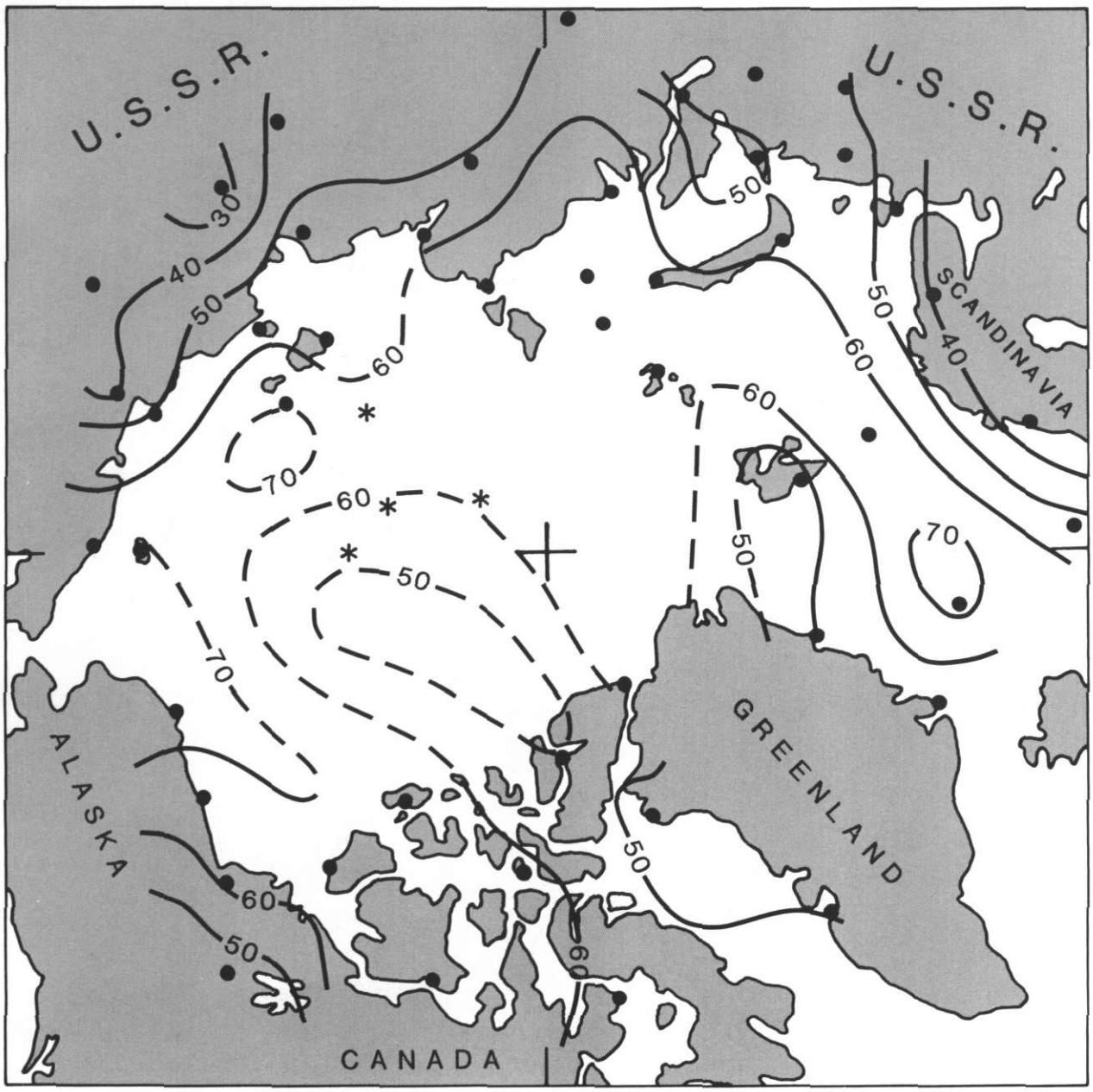

Figure E-7. Frequency of Elevated Inversions (%) for Spring.

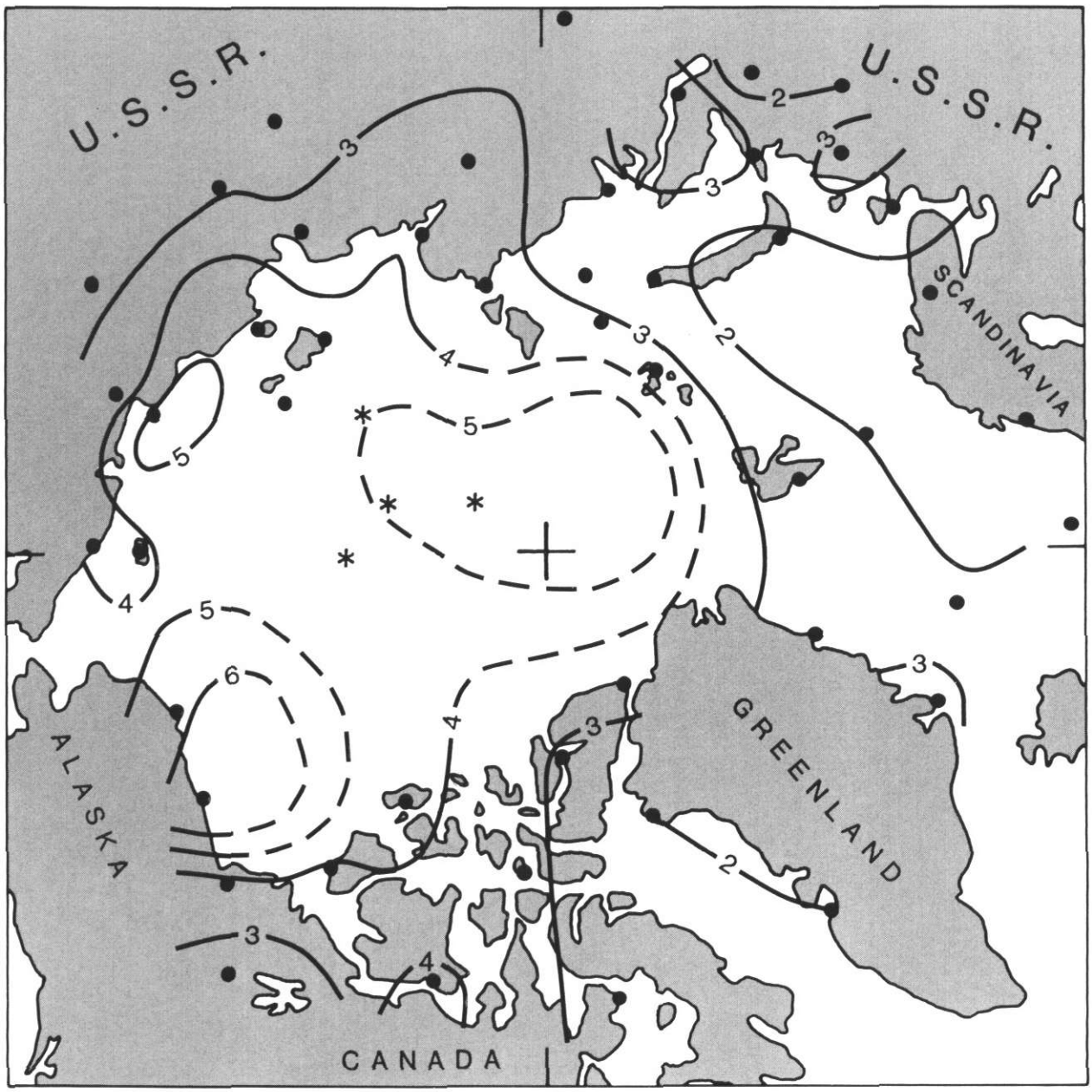

Figure E-8. Median Temperature Difference Across Inversion (°C) for Spring.

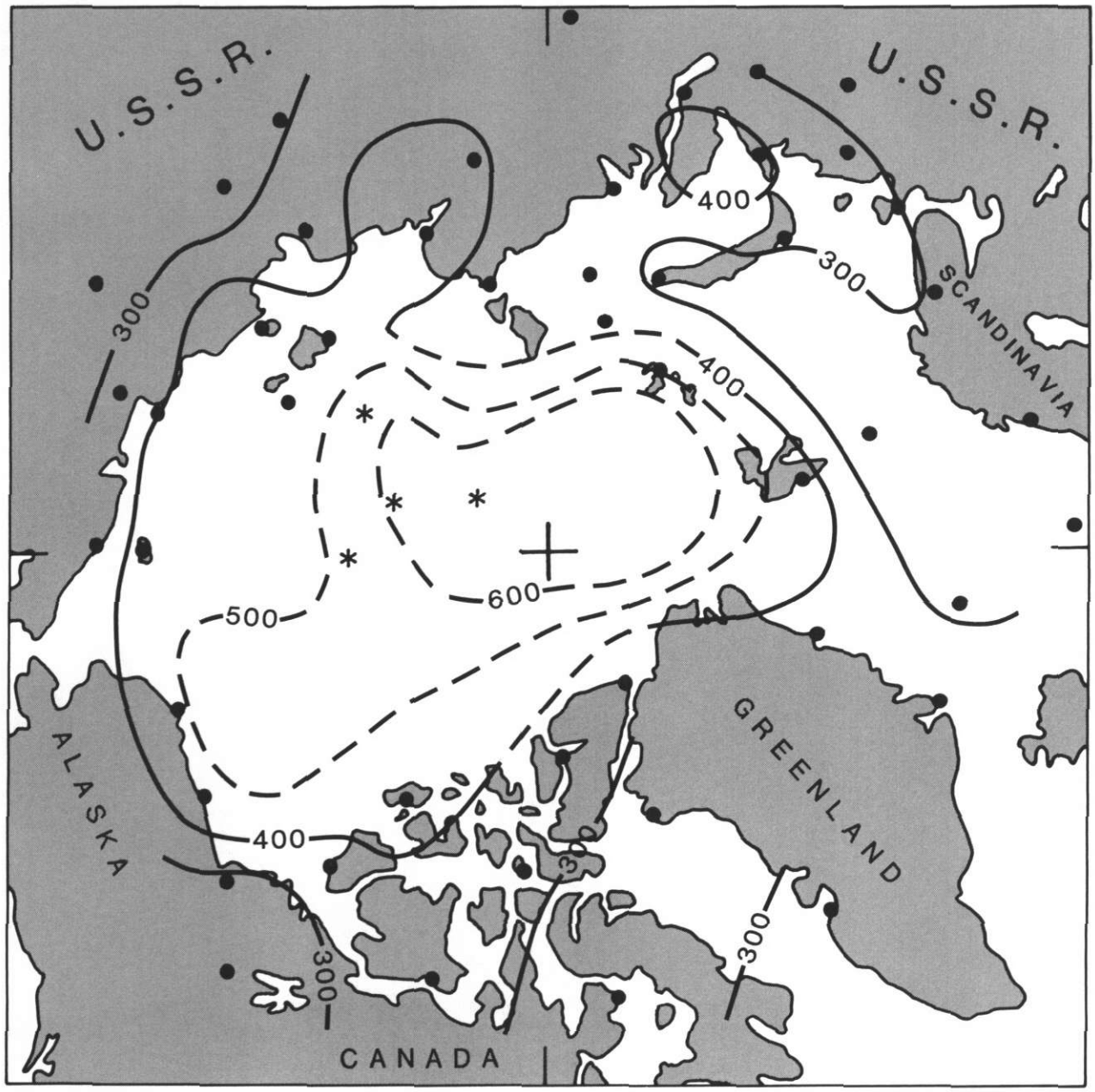

Figure E-9. Median Inversion Depth (m) for Spring.

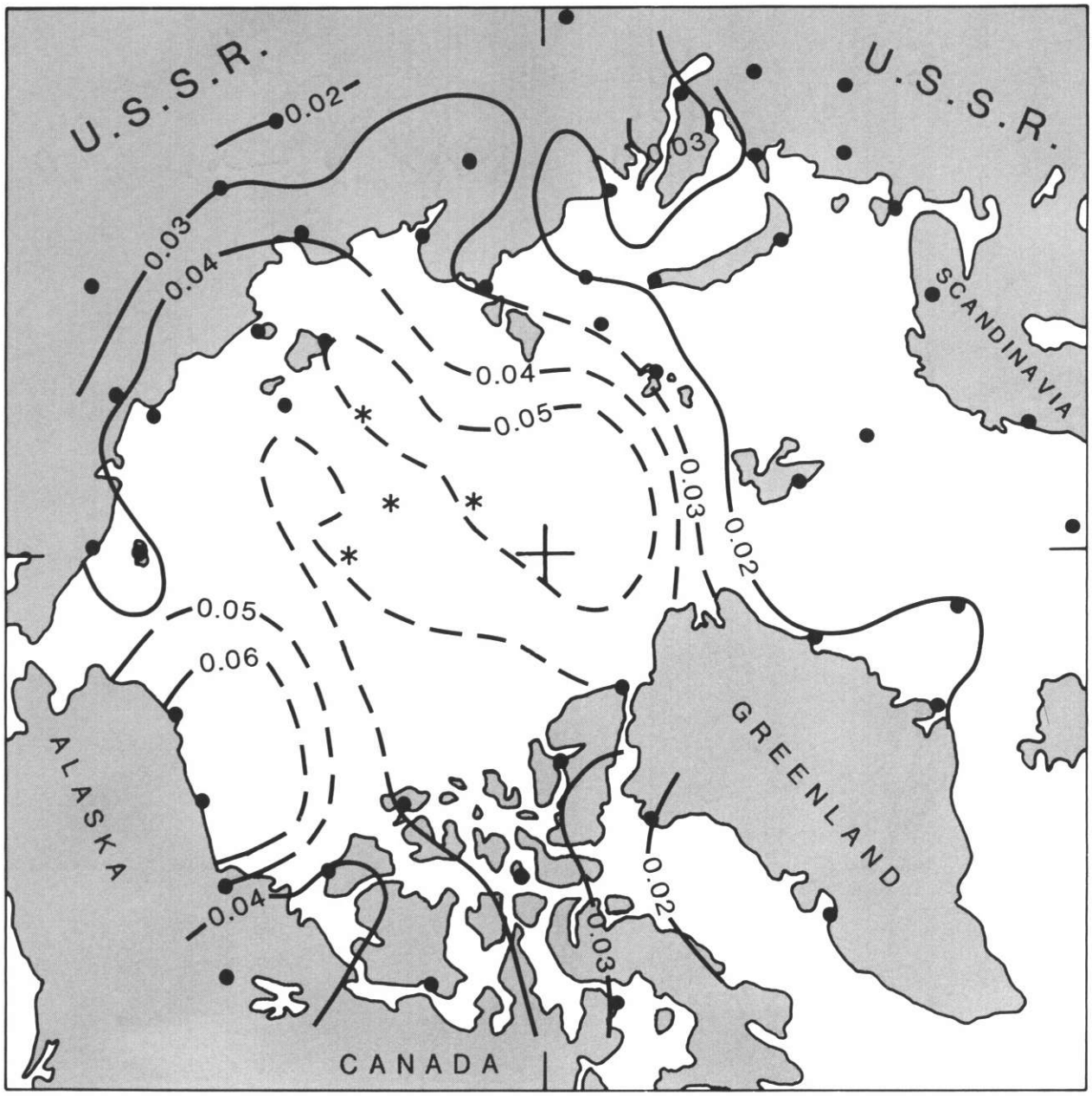

Figure E-10. Median Inversion Intensity ($\Delta T^2/m$) for Spring.

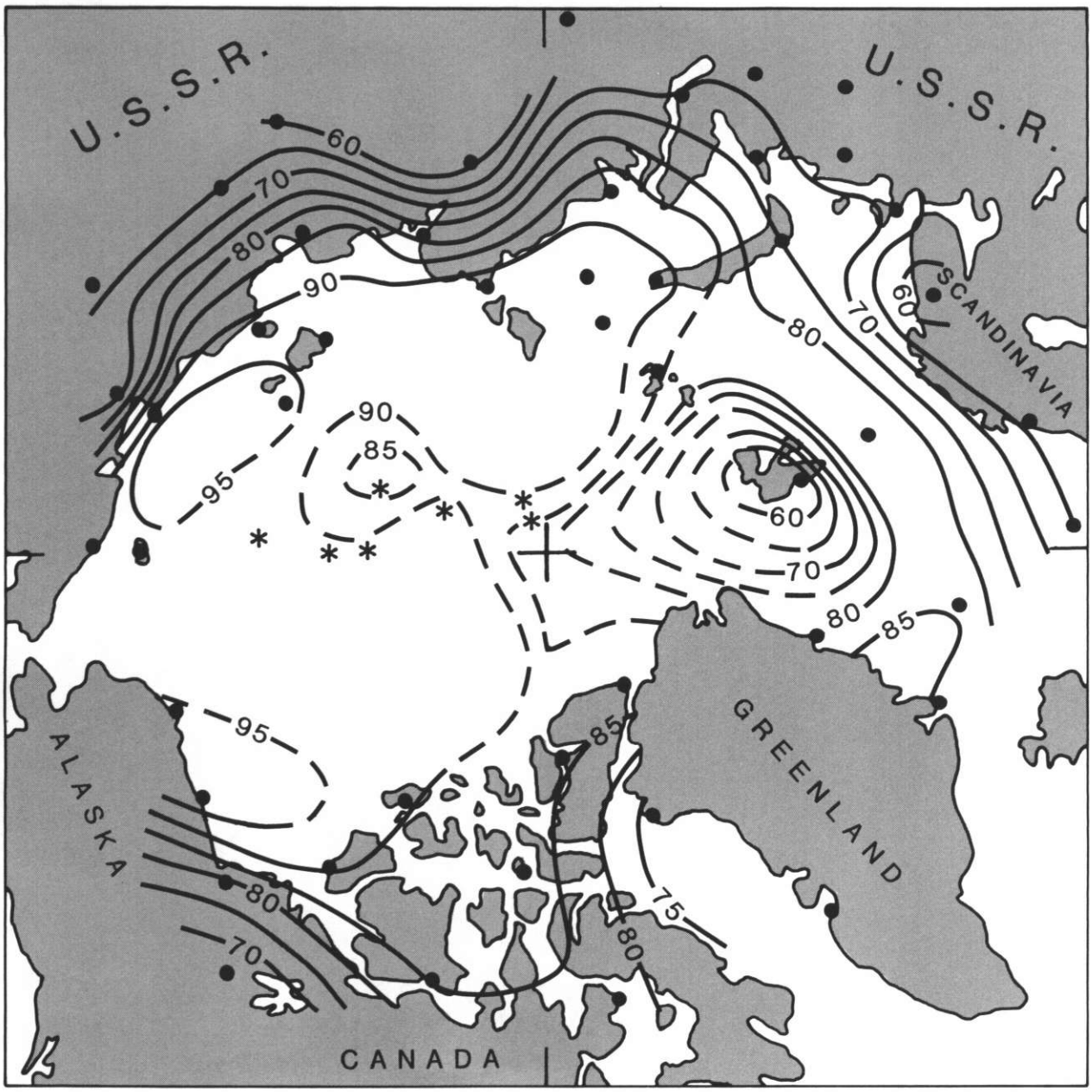

Figure E-11. Frequency of Inversions (%) for Summer.

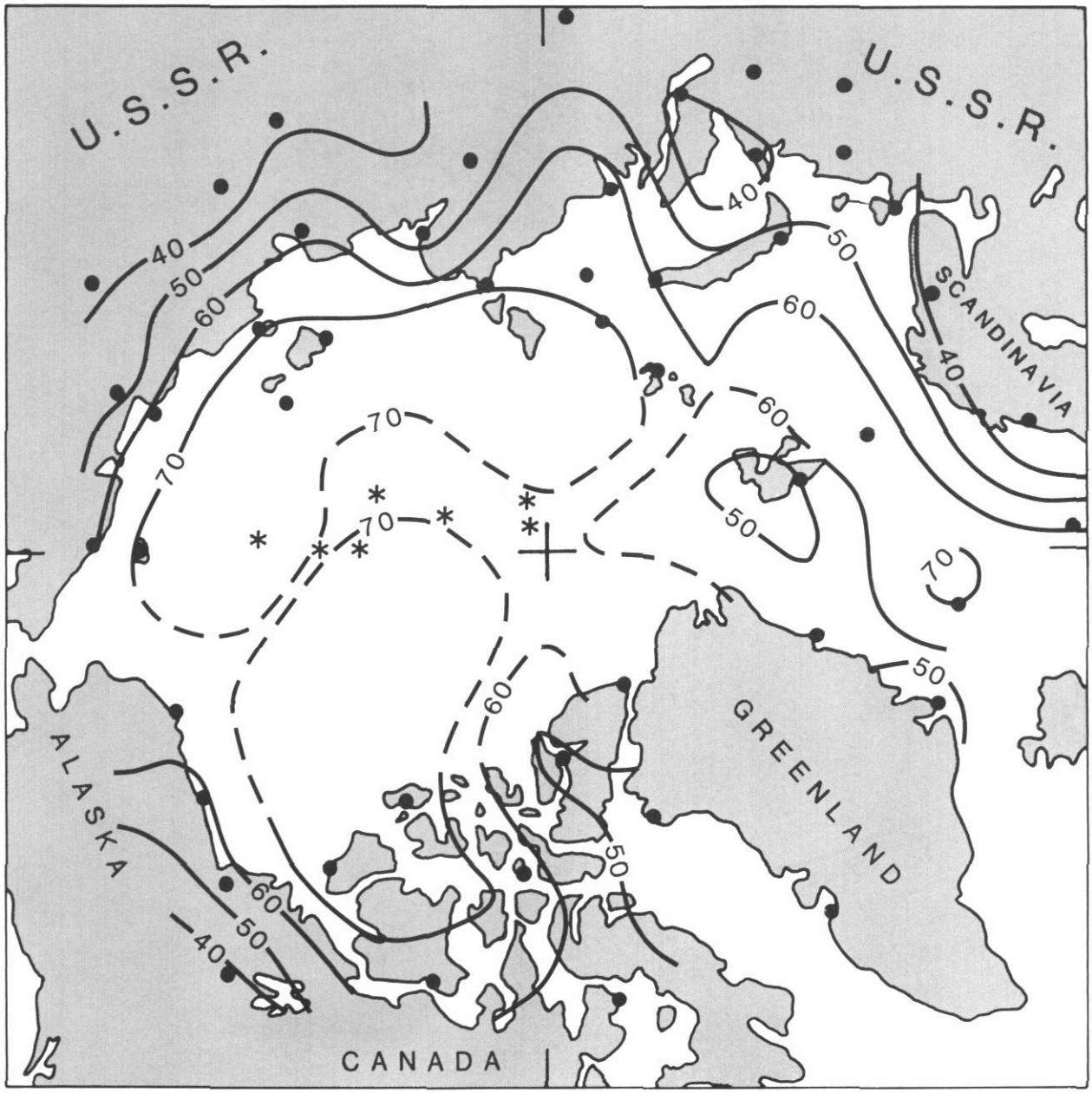

Figure E-12. Frequency of Elevated Inversions (%) for Summer.

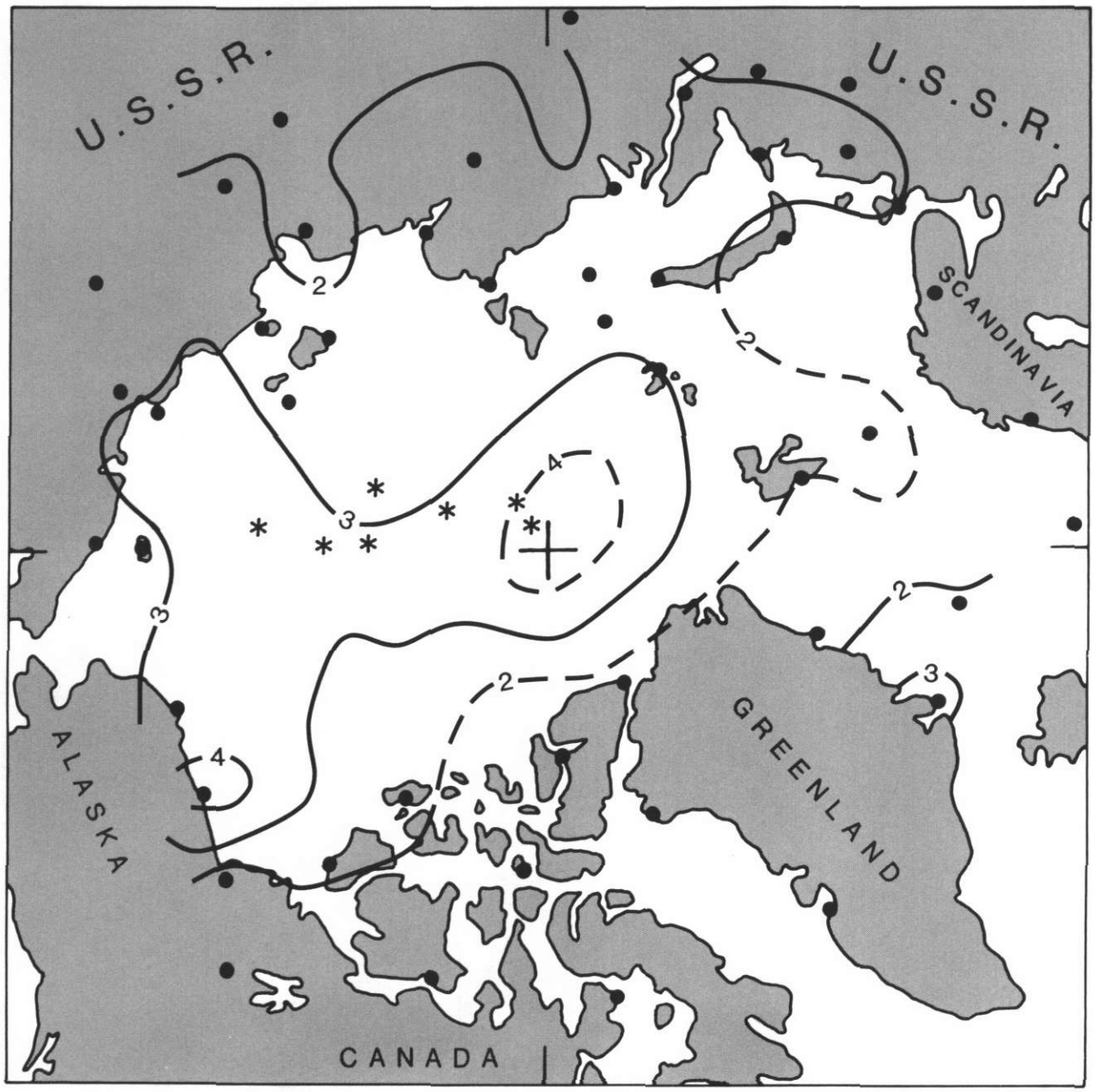

Figure E-13. Median Temperature Difference Across Inversion (°C) for Summer.

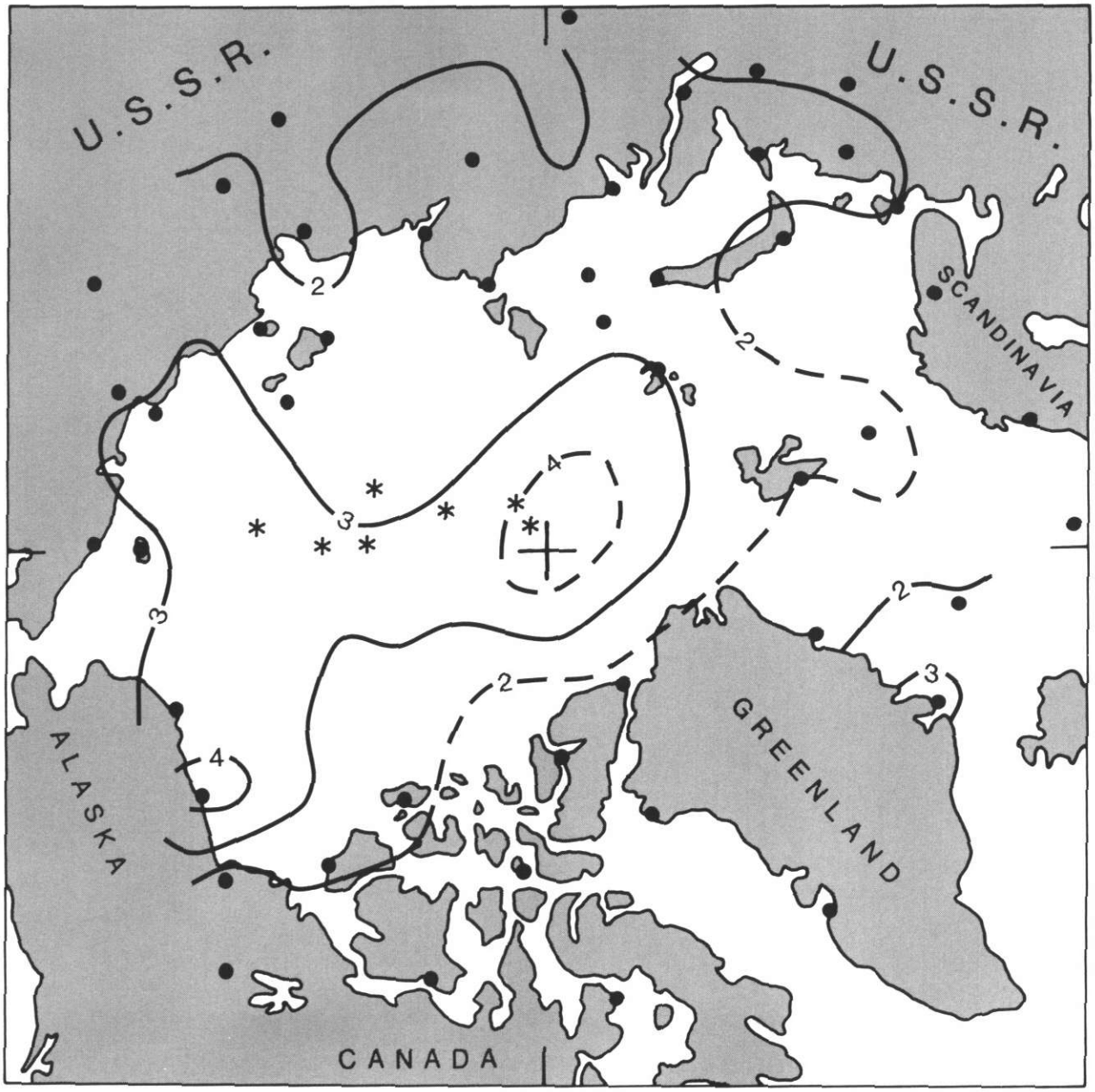

Figure E-13. Median Temperature Difference Across Inversion (°C) for Summer.

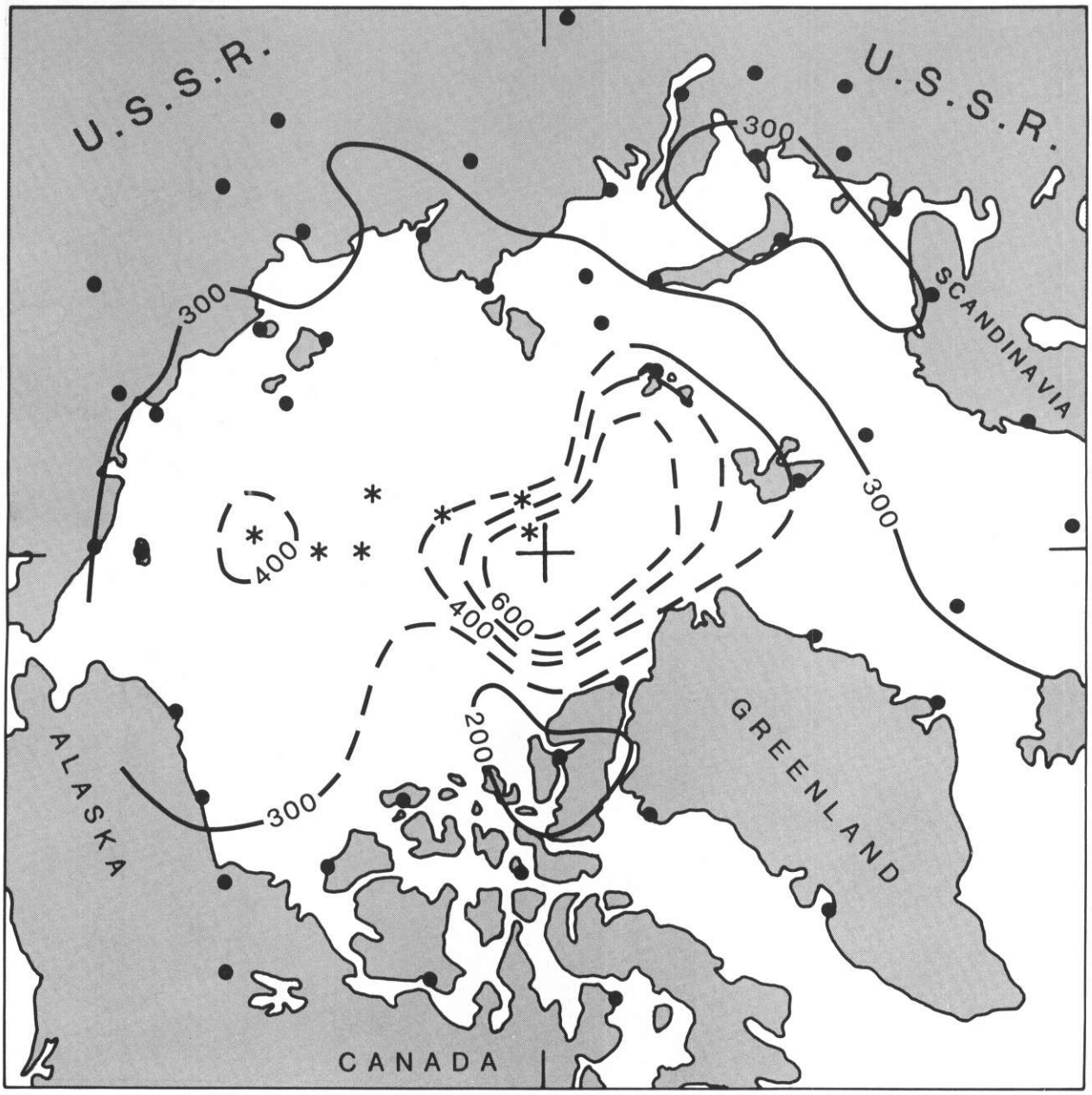

Figure E-14. Median Inversion Depth (m) for Summer.

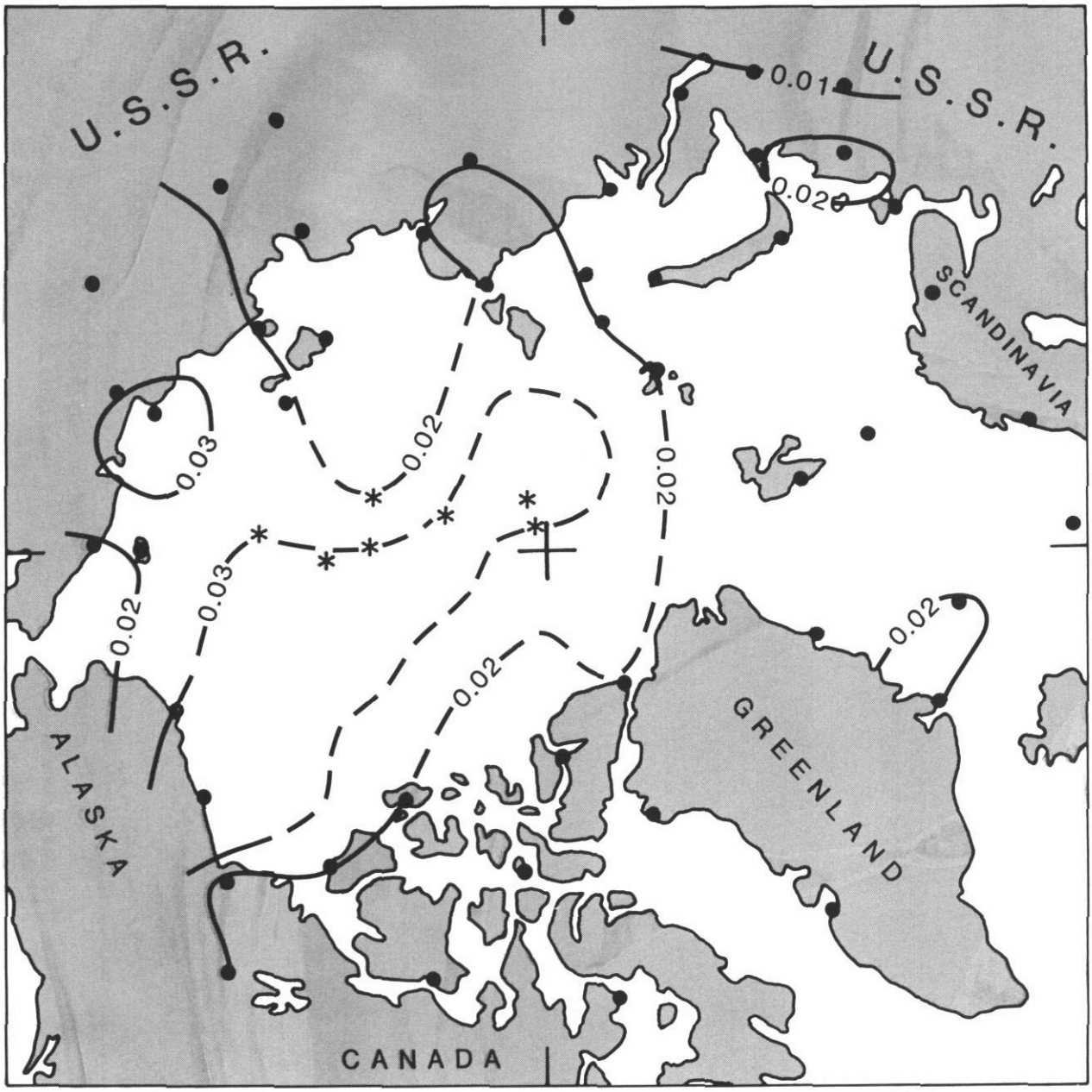

Figure E-15. Median Inversion Intensity ($\Delta T^2/m$) for Summer.

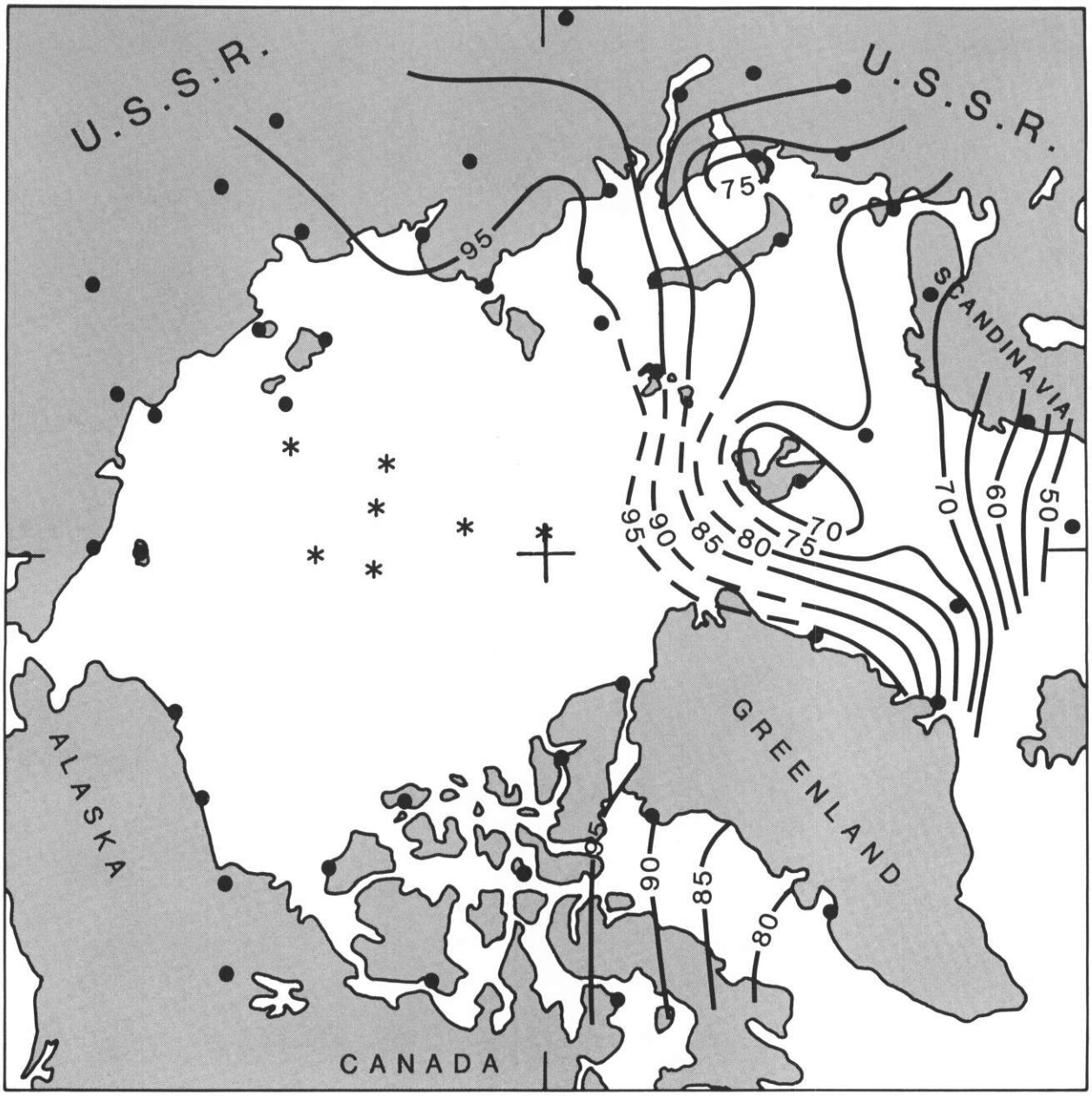

Figure E-16. Frequency of Inversions (%) for Autumn.

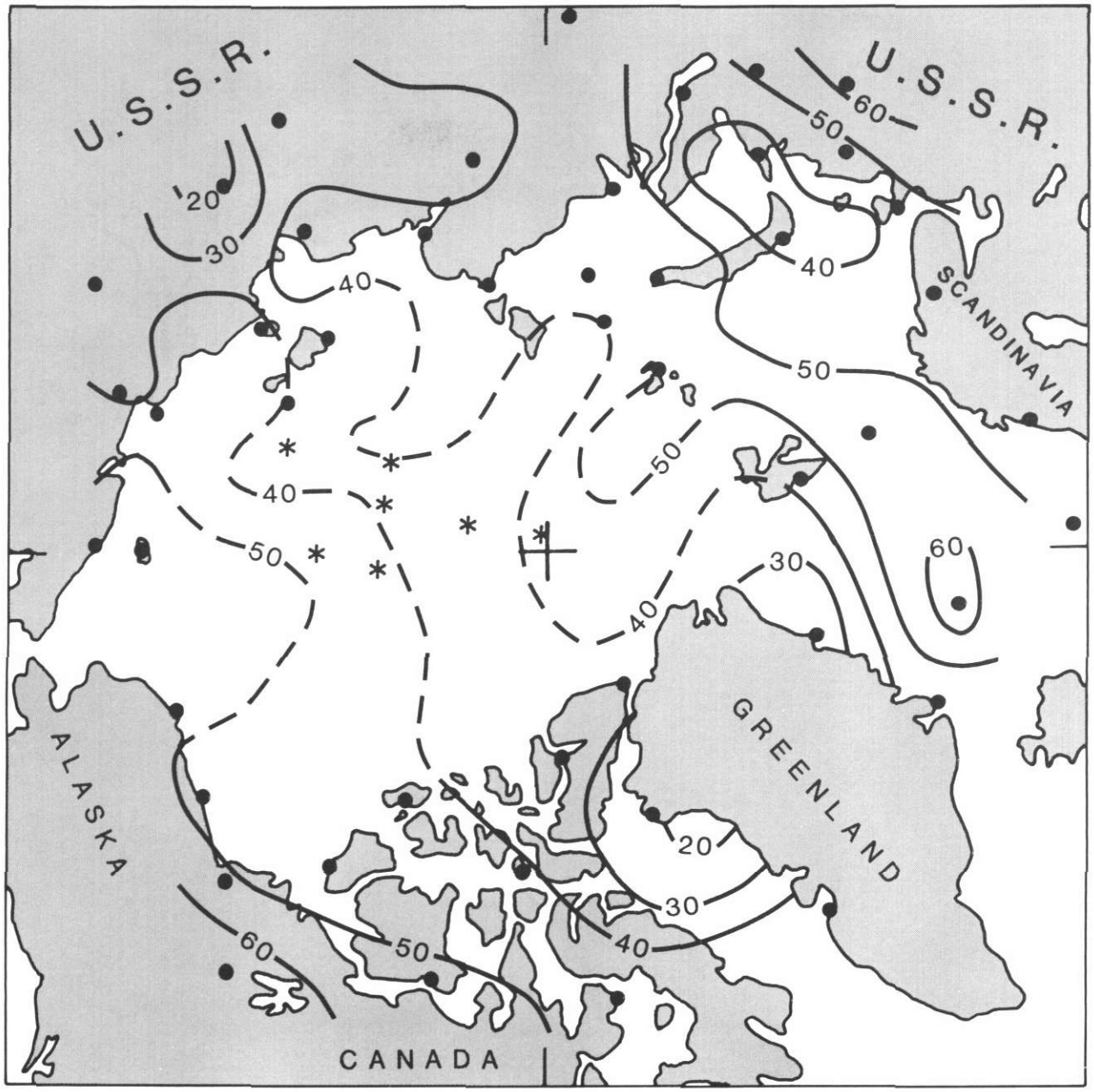

Figure E-17. Frequency of Elevated Inversions (%) for Autumn.

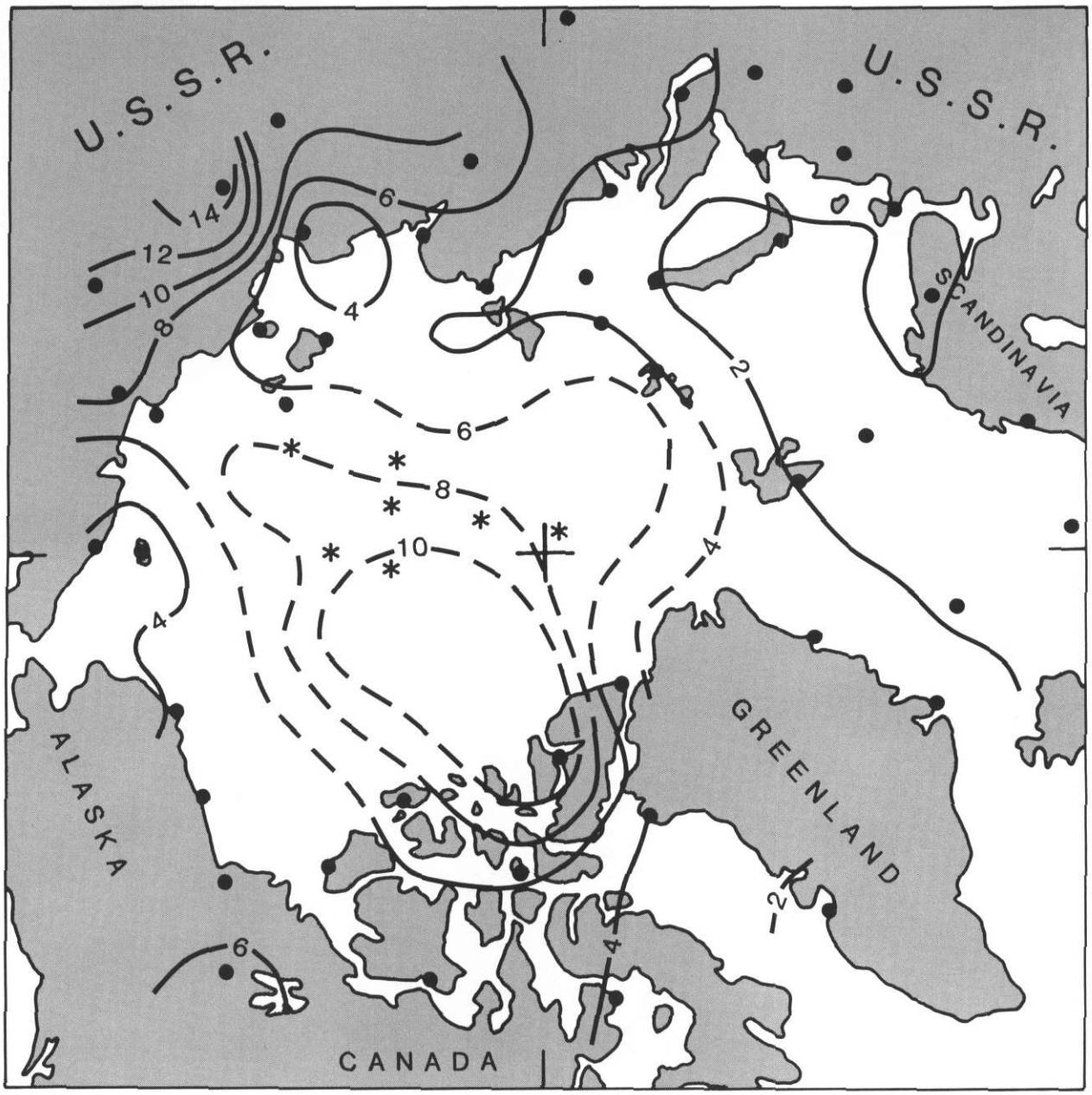

Figure E-18. Median Temperature Difference Across Inversion (°C) for Autumn.

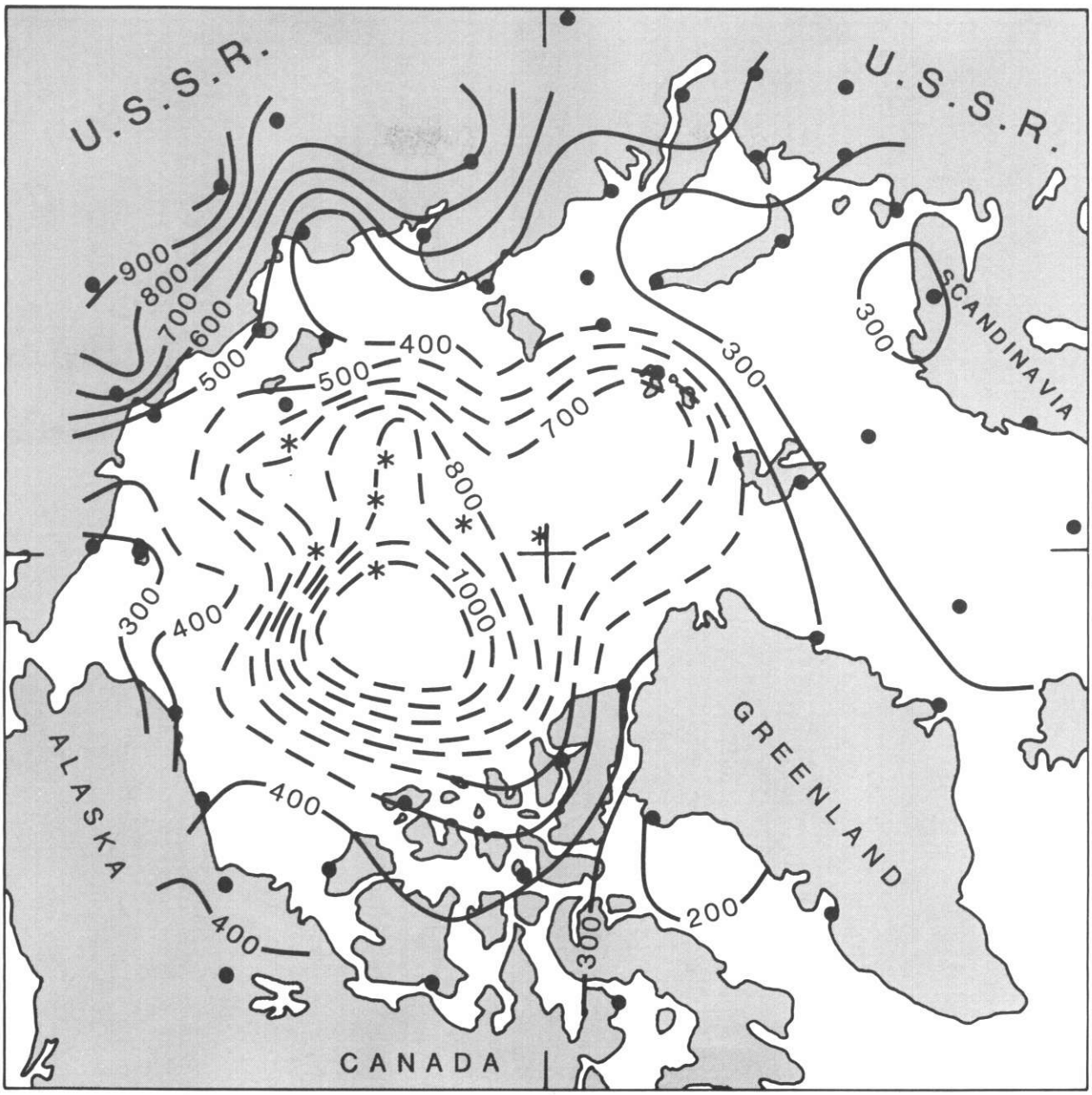

Figure E-19. Median Inversion Depth (m) for Autumn.

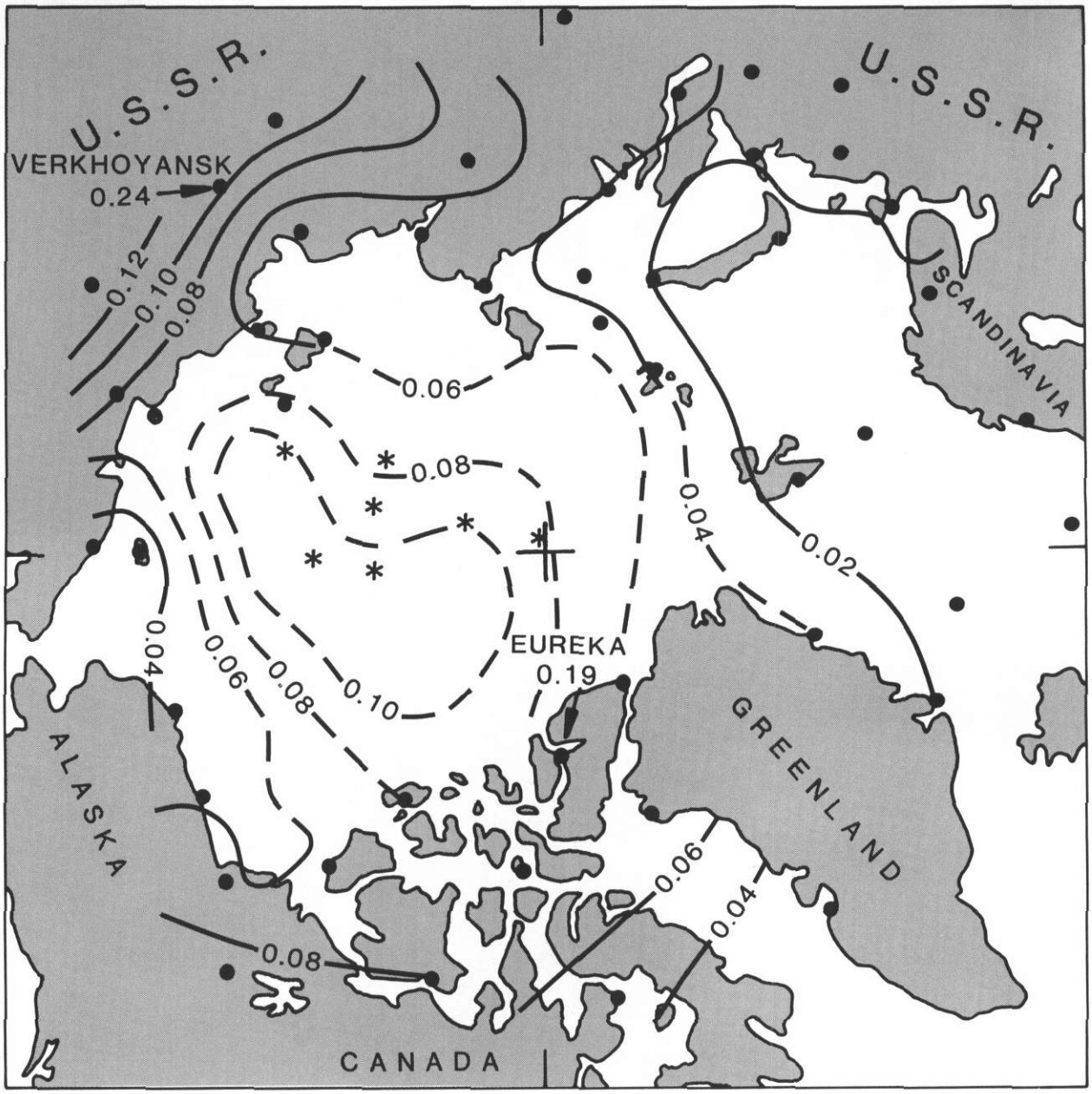

Figure E-20. Median Inversion Intensity ($\Delta T^2/m$) for Autumn.

STATION LISTING

	Lat(N)	Long	Elev(m)	Soundings	Station
Eurasian					
1	69.77	61.68E	53	6005	Amderma
2	78.07	14.22E	18	4991	Barentsburg
3	74.50	19.00E	18	7448	Bjornova
4	67.25	14.48E	8	7347	Bodo
5	71.58	128.92E	2	7200	Bukhta Tiksi
6	71.98	102.47E	32	4384	Khatanga
7	72.38	52.73E	19	4904	Malye Karmakuly
8	68.97	33.05E	57	6395	Murmansk
9	77.72	104.28E	12	6298	Mys Cheliuskin
10	68.47	73.60E	5	5736	Mys Kamenny
11	68.92	179.28W	4	7299	Mys Schmidt
12	73.18	143.93E	23	7068	Mys Shalaurova
13	76.95	68.58E	8	5586	Mys Zhelania
14	67.65	53.02E	7	7068	Narjan Mar
15	68.75	161.30E	23	7400	Nizhnie Krestiy/Cerski
16	70.63	162.40E	38	6881	Ostrov Chetyrekhstolbo
17	73.52	80.33E	45	5473	Ostrov Dikson
18	80.62	58.05E	20	6629	Ostrov Heisa
19	76.00	137.90E	13	7024	Ostrov Kotelny
20	74.67	112.98E	32	6519	Ostrov Preobrazhenia
21	77.60	82.23E	22	5735	Ostrov Uedinenia
22	79.50	76.98E	8	6137	Ostrov Vise
23	70.97	178.55W	2	6502	Ostrov Vrangelya
24	76.15	152.83E	14	6376	Ostrov Zohova
25	65.12	57.22E	54	6530	Pechora
26	66.53	66.55E	18	6031	Sale-Khard (Obdorsk)
27	67.88	44.17E	7	6354	Sojna
28	65.78	87.95E	38	6290	Turukhansk
29	67.55	133.38E	137	5033	Verkhoyansk
30	66.77	123.40E	82	6418	Zhigansk
31	65.73	150.90E	43	1974	Zyrianka
32	70.93	8.67W	9	6143	Jan Mayen
Greenland					
33	76.53	68.75W	77	5437	Thule
34	76.77	18.77W	11	5711	Danmarkshavn
35	70.42	21.97W	42	2772	Kap Tobin
36	68.70	52.75W	47	6677	Egedesminde

STATION LISTING (Concluded)

	Lat(N)	Long	Elev(m)	Soundings	Station
Moored Ship					
37	66.00	2.00E	0	6283	Ship "M"
U.S./Canada					
38	68.78	81.25W	10	6421	Hall Beach
39	74.72	94.98W	67	6371	Resolute
40	82.50	62.33W	63	6488	Alert
41	80.22	86.18W	10	6301	Eureka
42	68.32	133.53W	68	6510	Inuvik
43	69.10	105.13W	27	6559	Cambridge Bay
44	65.28	126.80W	73	6478	Norman Wells
45	76.23	119.33W	20	6351	Mould Bay
46	71.97	124.73W	86	6470	Sachs Harbour
47	71.28	156.77W	7	6864	Barrow Island
48	70.13	143.57W	2	6800	Barter Island

Total land station soundings = 295,671

Drifting Station Data:

NP-22, NP-26, NP-28

Total drifting station soundings = 2,994

References:

Belmont, A. D., 1958: Lower tropospheric inversions at ice island T-3. *Polar Atmospheric Symposium, Part 1 Meteorology Section,* Pergamon Press, London, 215–284.

Kahl, J. D., 1990: Characteristics of the low-level temperature inversion along the Alaska Arctic coast. *Int. J. Clim., 10,* 537–548.